Water Research 186 (2020) 116355

Contents lists available at ScienceDirect

Water Research

journal homepage: www.elsevier.com/locate/watres

Nitrate loading projection is sensitive to freeze-thaw cycle representation

Qianfeng Wang[a], Junyu Qi[b,*], Jia Li[c], Jefferson Cole[c], Stephanie T. Waldhoff[a], Xuesong Zhang[b,*]

[a] Joint Global Change Research Institute, Pacific Northwest National Laboratory and University of Maryland, College Park, MD 20740, USA
[b] Earth System Science Interdisciplinary Center, University of Maryland, College Park, 5825 University Research Ct, College Park, MD, 20740, USA
[c] U.S. Environmental Protection Agency, 1200 Pennsylvania Avenue, NW (6207 A), Washington, DC 20460, USA

ARTICLE INFO

Article history:
Received 19 June 2020
Revised 20 August 2020
Accepted 28 August 2020
Available online 29 August 2020

Keyword:
Climate change
Freeze-thaw cycle
Nitrate runoff
Nitrate leaching
Water quality

ABSTRACT

Climate change can have substantial impacts on nitrogen runoff, which is a major cause of eutrophication, harmful algal blooms, and hypoxia in freshwaters and coastal regions. We examined responses of nitrate loading to climate change in the Upper Mississippi River Basin (UMRB) with an enhanced Soil and Water Assessment Tool with physically based Freeze-Thaw cycle representation (SWAT-FT), as compared with the original SWAT model that employs an empirical equation. Driven by future climate projections from five General Circulation Models (GCMs) from 1960 to 2099 under the Representative Concentrations Pathways (RCP) 8.5 scenario, we analyzed changes in riverine nitrate loadings, as well as terrestrial surface and subsurface contributions of the UMRB in the 21st century relative to the baseline period of 1960–1999. By the end of the 21st century, the original SWAT model predicted about a 50% increase in riverine nitrate loadings which is nearly twice as much as that estimated by SWAT-FT (ca. 25%). Such a large difference in projected nitrate changes can potentially mislead mitigation strategies that aim to reduce nitrogen runoff from the UMRB. Further analysis shows that the difference between the original SWAT model and SWAT-FT led to substantial discrepancies in the spatial distribution of surface and subsurface nitrate loadings in the UMRB. In general, SWAT-FT predicted more nitrate leaching for northwestern parts of the UMRB which are more sensitive to freeze-thaw cycle, mainly because SWAT-FT simulated less frequent frozen soils. This study highlights the importance of using physically based freeze-thaw cycle representation in water quality modeling. Design of future nitrogen runoff reduction strategies should include careful assessment of effects that land management has on the freeze-thaw cycles to provide reliable projection of water quality under climate change.

1. Introduction

It is largely in agreement that global warming due to increasing carbon dioxide and accumulating other greenhouse gasses would likely continue in the 21st century (Nunes et al., 2008). Global warming can generate higher evapotranspiration rates causing dramatic changes in precipitation pattern worldwide (Buytaert et al., 2010), thereby adding uncertainty in regional water resources variability (Middelkoop et al., 2001). Climate change can alter terrestrial nitrogen cycles and riverine nitrate fluxes. High nitrate concentrations in water bodies can deteriorate water quality, degrade ecological functions of aquatic systems, impair aquatic biota, and pollute underground water (Miller et al., 2017; Zhang et al., 2008b; c). Nitrate in certain freshwater systems can boost phytoplankton growth and algal blooms and result in eutrophication (Schindler, 2012), which can further deplete the oxygen in water and cause reduction of aquatic biodiversity and fish stock (Kendall, 1998). Hydrologic models are often used to assess the potential impacts of climate change on the water resources availability and water quality (Hagemann et al., 2013). Model credibility depends on how accurately the model represent real world processes. Most hydrologic models, however, have underrepresented freeze-thaw cycles which is amongst the processes most sensitive to climate change (Bakir and Zhang, 2008; Wu et al., 2014). It has been pointed out that misrepresentation of freeze-thaw cycles tends to enlarge model prediction uncertainty under future climate change scenarios (Guo and Wang, 2013; Yang et al., 2007).

Over one-third of the global land surface experiences freeze-thaw cycle (Kimball et al., 2001), and seasonally frozen soils oc-

* Corresponding authors.
E-mail addresses: junyuqi@umd.edu (J. Qi), xzhang14@umd.edu (X. Zhang).

https://doi.org/10.1016/j.watres.2020.116355
0043-1354/

cupy nearly 60% of the land surface of the Northern Hemisphere (Hagemann et al., 2013). Soil thermal status can potentially alter hydrological cycles and associated water quality processes at the regional/global scales (Wu et al., 2018). The seasonal freeze-thaw cycle of soils has significant influences on water infiltration from precipitation/snowmelt, water migration in soils, and nutrient movement in terrestrial environments (Ouyang et al., 2013; Yi et al., 2014; Zhao et al., 2013). The freezing process can cause soil water movement into freezing front resulting in elevated soil water content and increased surface runoff (Zhang and Sun, 2011). The thawing process can promote infiltration and resultant groundwater discharge leading to increased nitrate leaching (Hentschel et al., 2008; Yu et al., 2011). Therefore, it is essential to investigate the nitrate loading from terrestrial environments and in streams in response to future climate changes through accounting for the freeze-thaw cycle in hydrological modeling.

Hydrological models are useful tools for assessing potential impacts of future climate change on nitrate migration from soils to streams. Comparison between eleven hydrological models indicated that the SWAT model was the most suitable model for simulating long term water quantity and quantity in agriculture dominance watersheds (Borah and Bera, 2003). The SWAT model has been used to simulate water quantity and quality in almost all large basins worldwide. However, its application has confronted many difficulties in cold regions affected by seasonal freeze-thaw cycle (Bakir and Zhang, 2008), because its simplified empirical soil temperature module does not represent well phase changes of water and take into account of snow insulation effects. This model deficiency tends to undermine its use for prediction of future climate change impacts (Guo and Wang, 2013; Yang et al., 2007).

The Upper Mississippi River Basin (UMRB) is a major nitrate source of eutrophication and hypoxia in the Gulf of Mexico (Rabalais et al., 1996). Although it only occupies 18% of the whole Mississippi River Basin (Moriasi et al., 2013), nitrate loadings from UMRB account for about 35% of total nitrate loadings to the Gulf of Mexico (Alexander et al., 1997), due to its intensive agriculture activities as one of the most productive areas in the U.S. Since most soils of UMRB are subject to seasonal freeze-thaw cycle, the assessment of best management practices to reduce nitrate loadings in the UMRB is subject to large uncertainty when using the SWAT model with the empirical soil temperature module. As important action plans are being framed and undertaken to reduce nitrogen runoff in the Mississippi River Basin (Plan, 2008), for example, reducing nitrate loading by 30% in the Gulf of Mexico (Mitsch et al., 1999), it is important to understand how freeze-thaw cycle representation in the SWAT model can influence nitrate simulation.

To our knowledge, there is a general lack of studies evaluating hydrological models with respect to the role of freeze-thaw cycle representation on nitrate loading simulation. Thus, we evaluated implications of freeze-thaw cycle representation for water quality modeling under future climate change conditions in the UMRB. Two versions of SWAT model were used, i.e. an enhanced SWAT model with a physically based Freeze-Thaw cycle representation (hereafter, SWAT-FT) and the original SWAT model with an empirical representation. A major driver for the current study is the large differences between the original SWAT model and SWAT-FT in simulating soil thermal status (Qi et al., 2019c). Multiple General Climate Models (GCMs) simulations of future climate under the Representative Concentration Pathways 8.5 scenario (RCP8.5) are employed. The objectives of this study are to: 1) analyze precipitation and air temperature trends projected by GCMs from 1960 to 2099 in the UMRB, 2) compare simulations of riverine nitrate fluxes between the original SWAT model and SWAT-FT from 1960 to 2099, 3) compare predicted nitrate loadings carried by surface and subsurface flow at the temporal and spatial scales between the original SWAT model and SWAT-FT, and 4) assess water quality in the UMRB under the impact of future climate change. Overall, we hope to improve our understanding of nitrate cycling processes influence by freeze-thaw cycle, and further inform decision makers to facilitate designing economically suitable agricultural practices and regulating water quality management strategy.

2. Materials and methods

2.1. Introduction to swat-ft

2.1.1. Empirical vs. physically based soil temperature modules

The SWAT model employs a simple soil temperature formula to represent soil freeze-thaw cycle (Neitsch et al., 2011a):

$$T_{soil}(z) = \gamma \cdot T'_{soil}(z) + (1-\gamma)\cdot\left[d\cdot\left(\bar{T}_{Air} - T_{sur}\right) + T_{sur}\right] \quad (1)$$

where, T_{soil} is the soil temperature at depth z on the current day, γ is a lag coefficient considering the effect of soil temperature (T'_{soil}) of the previous day on T_{soil}, d is accounting for the effect of soil depth on soil temperature, $\bar{T}_{Air}$ is the average annual air temperature, and T_{sur} is the soil surface temperature. This simple empirical soil temperature module was found to severely underestimate soil surface temperature during winter for cold regions (Qi et al., 2016b, 2019c). In addition, snow insulation and protective effects were not well simulated by the empirical module (Qi et al., 2016a; Zhang, 2005). Most importantly, because the empirical module does not simulate water phase changes in the soil profile, the original SWAT model does not explicitly simulate freeze-thaw cycle. As a result, hydrological and biogeochemical processes coupled with freeze-thaw cycle cannot be accurately simulated in cold regions with seasonal snow cover (Zhang et al., 2008a).

To address this problem, Qi et al. (2016b) have developed a physically-based soil temperature module within the SWAT model to better simulate the insulating and protective effects of snow and phase changes of soil water, and successfully validated the improved SWAT model (Qi et al., 2016a; b; Qi et al., 2019b, 2019c). For the physically-based method, soil temperature can be obtained according to the following formula (Qi et al., 2016b):

$$\frac{\partial T}{\partial t} = \frac{\partial}{\partial x}\left(\frac{k}{C}\cdot\frac{\partial T}{\partial x}\right)\frac{s}{C} \quad (2)$$

where, T denotes the soil temperature (°C), t is time increments (in days), k denotes soil thermal conductivity (J cm^{-1} d^{-1} °C^{-1}), C denotes soil heat capacity (J cm^{-3} °C^{-1}), x denotes downward depth from soil/snow surface (cm), and s denotes soil latent heat in source or sink (J cm^{-3} d^{-1}). Eq. (2) was converted to a fully-implicit discretized form solved with a tridiagonal-matrix algorithm. Vertically, the simulation domain was defined as extending from the air-soil or air-snow interface (surface boundary) to the damping depth (bottom boundary) (Fig. 1). When snow accumulated on the ground, the snow cover was treated as a single layer (Fig. 1). The surface boundary temperature was calculated based on an energy balance algorithm (Hillel, 1980). The bottom boundary was defined at the damping depth, and the temperature at the damping depth was determined following the method of Steppuhn (1981). The thermal conductivity of snow was calculated as a function of snow density according to Sturm et al. (1997), and soil thermal conductivity of both unfrozen and frozen soils were determined based on the method developed by Johansen (1975). The volumetric heat capacity for soils was calculated as the volumetric weighted mean of specific heat capacity of soil constituents, while for snow it was calculated based on Verseghy (1991). Volumetric soil ice and water content were calculated according to the release of energy during the freezing of liquid water and the absorption of energy during the melting of ice (Fig. 1). A soil layer froze when its temperature reached or fell below 0°C and thawed when its temperature exceeded 0°C (Fig. 1).

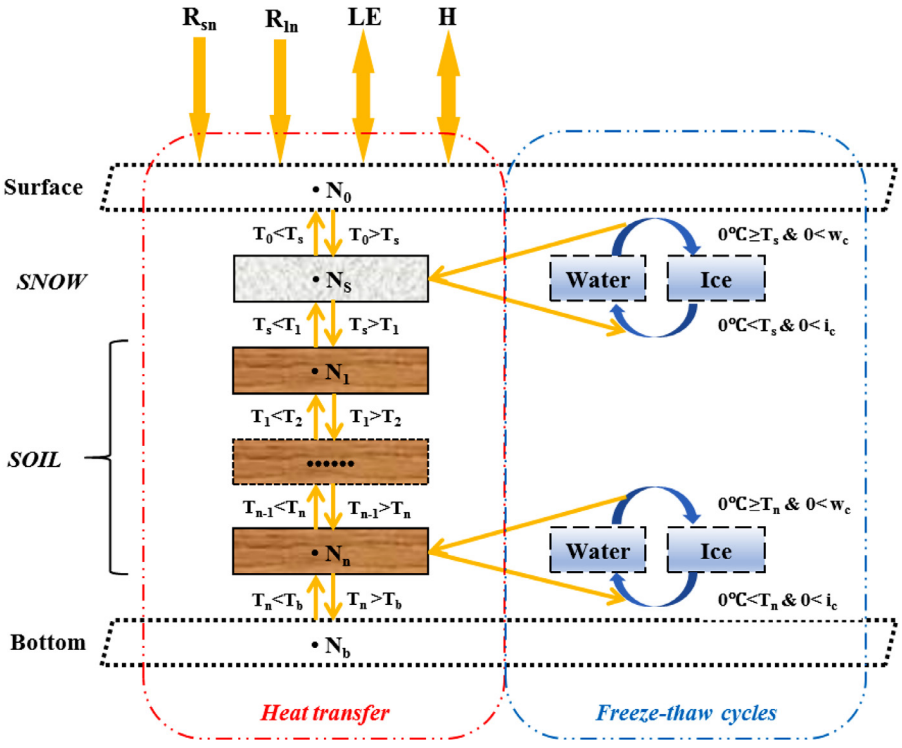

Fig. 1. Schematic flowchart of coupled heat transfer and freeze-thaw cycles in snow and soil layers. R_{sn} is the net solar radiation, R_{ln} is the net longwave radiation, LE is the latent heat flux, H is the sensible heat flux, T_n is the temperature for nth node (N_0 and N_b are the surface and bottom nodes; N_s is the node at the center of the snow layer; N_1 to N_n are nodes centered at each soil layer), and i_c and w_c are ice and water content in each soil layer. Yellow arrows indicate heat transfer processes and blue arrows indicate mass transfer processes.

2.1.2. Nitrate cycling coupled with soil hydrology

Soil biogeochemical processes were simulated by a CENTURY-based C/N cycling module which was recently incorporated into the SWAT model by Zhang et al. (2013). The module has proven to simulate soil C/N transformation and C/N loading/emissions from agricultural soils better than the original SWAT's soil biogeochemistry module (Qi et al., 2020; Yang et al., 2017; Zhang, 2018; Zhang et al., 2013). The CENTURY-based C/N cycling module separates the soil organic matter and residue into five pools, including structural litter, metabolic litter, microbial biomass, and slow and passive humus, and simulates addition, decomposition, transformation, and removal of each SOM-residue pool present in surface and subsurface soil layers (Zhang et al., 2013). Mineralization of organic matter and immobilization of nitrate and ammonium are microbially mediated and controlled by different pools' turnover rates and abiotic factors, such as soil temperature, soil water content, tillage enhancement, oxygen availability, and soil texture (Zhang et al., 2013). We also added CENTURY-based algorithms to simulate N_2O and N_2 emissions generated via denitrification and nitrification (Parton et al., 1996; Yang et al., 2017).

Nitrate load to rivers is associated with surface runoff, leaching, and subsurface runoff (including lateral flow, tile flow, and baseflow as shown in Fig. 2. In the SWAT model, nitrate concentration is multiplied by the water moving in each pathway to obtain the mass of nitrate lost from the soil layer and aquifer (Neitsch et al., 2011b). In cold regions, partitioning of surface and subsurface runoff is affected by soil thermal status during winter and the snow melting seasons (Fig. 2). Thus, we anticipate that soil freeze-thaw cycles will have significant impacts on nitrate loadings via different water flow pathways.

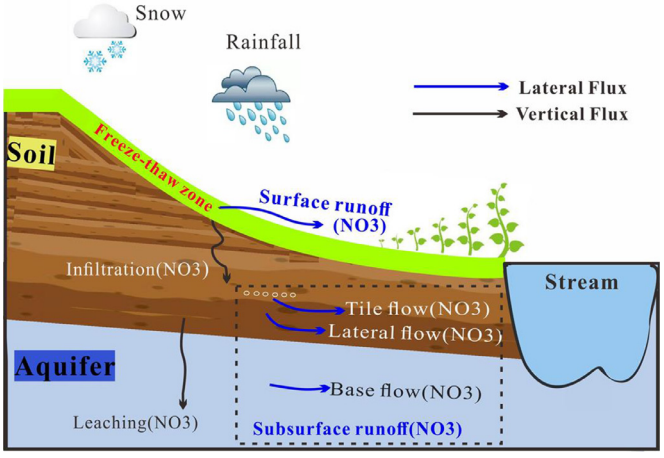

Fig. 2. Schematic diagram of partitioning of surface and subsurface nitrate runoff as affected by freeze-thaw cycles in cold regions. Subsurface runoff includes soil lateral flow, tile flow, and baseflow for the present study.

2.2. Study area and data collection

2.2.1. Upper Mississippi river basin

The UMRB, covering approximately 492,000 km^2, is an important upstream watershed within the Mississippi River Basin (MRB) (ca. 18% of MRB) (Moriasi et al., 2013). The UMRB extends from Lake Itasca in Minnesota to the Ohio River of north of Cairo, Illinois (Fig. 3). Cropland, predominantly corn and soybean, accounts for ca. 50% of the total area of the UMRB (Deb et al., 2015). Due to the

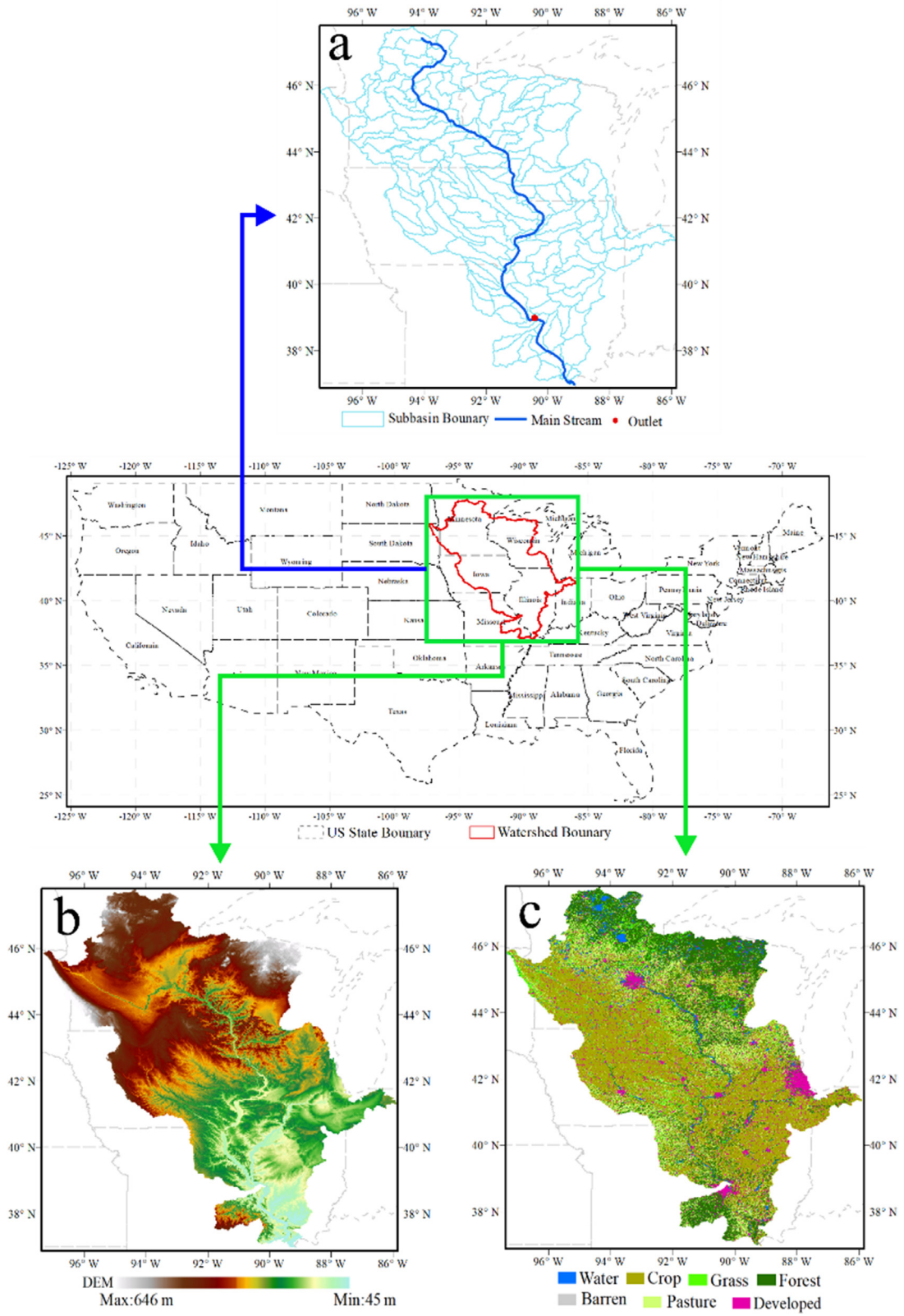

Fig. 3. Location of the Upper Mississippi River Basin and its elevation distribution, land use types, and subbasins divided based on eight-digit hydrologic unit catalog. (a: subbasins and mainstream, b: elevation, and c: land use types).

intensive agriculture activities, the UMRB contributed about 43% of the total nitrate loadings to the Gulf of Mexico between 2001 and 2005 leading to severe hypoxia (Panagopoulos et al., 2014). Soils in the UMRB consist mainly of silty loam and loam soils, and are subject to seasonal freeze-thaw cycle (Qi et al., 2019c). Elevation varies between 45 and 645 m, and flat and rolling terrains are dominant (Deb et al., 2015). The UMRB has as a sub-humid continental climate (Panagopoulos et al., 2014), with average annual precipitation of 900 mm and ca. 75% of annual precipitation falling in the growing season (between April and October). The UMRB has extensive subsurface tile drainage systems for the purpose of soil conservation and improving crop production (Deb et al., 2015; Wu et al., 2012).

2.2.2. Model setup and data collection

A previously developed SWAT project for the UMRB has been successfully tested for water quantity and quality simulations under ungauged conditions (Qi et al., 2019a, 2019c, 2020; Srinivasan et al., 2010). The main input data including Digital Elevation Model (DEM), weather data, land use, and soil data for the SWAT-UMRB project are shown in Table 1. The UMRB is divided into 131 subbasins based on the eight-digit United States Geological Survey (USGS) hydrologic unit codes (HUCs) (Srinivasan et al., 2010). Management operation data in UMRB such as tile drainage, tillage, crop rotation, irrigation, and fertilizer application are obtained according to multi-sources (Srinivasan et al., 2010). Monthly observed stream flow and nitrate loading data used for performance evaluation of two different versions of SWAT model were derived from U.S. Geological Survey (USGS) gage station # 05,587,450 (Grafton, Illinois) during 1997–2007.

2.2.3. Climate change data

We collected and compiled daily precipitation, solar radiation, relative humidity, maximum/minimum air temperature, and wind speed data from five Coupled Model Intercomparison Project Phase 5 (CMIP5) GCMs, namely GFDL, HadGEM2, IPSL, MIROC and NorESM1, which have been widely used in climate change studies (Table 2). The future projection dataset has been corrected with observed data using the bias-correction and spatial-downscaling approach (Yang et al., 2019). We chose the RCP 8.5 to assess impact of climate change scenarios on nitrate loading in the UMRB reflecting the business-as-usual emissions scenario (i.e., greenhouse gas emissions will continue to rise throughout the 21st century).

2.3. Model evaluation

2.3.1. Model performance on simulating stream flow and nitrate loadings

The only difference between the two models is that SWAT-FT used the physically based soil temperature module to represent soil freeze-thaw cycles. All other hydrological and biogeochemical algorithms remained the same. Model performances on simulating stream flow and nitrate loadings at the outlet of UMRB were evaluated based on three widely used model efficiency coefficients, including Nash-Sutcliffe efficiency (*NS*) (Nash and Sutcliffe, 1970), coefficient of determination (R^2), and percentage bias (*PBIAS*):

$$NS = 1 - \frac{\sum_{i=1}^{n}(O_i - P_i)^2}{\sum_{i=1}^{n}(O_i - \bar{O})^2} \tag{3}$$

$$R^2 = \left(\frac{\sum_{i=1}^{n}\left(O_i - \bar{O}\right)\cdot\left(P_i - \bar{P}\right)^2}{\sqrt{\sum_{i=1}^{n}(O_i - \bar{O})^2 \cdot \sum_{i=1}^{n}(P_i - \bar{P})^2}}\right)^2 \tag{4}$$

$$PBIAS = \frac{\left(\bar{P} - \bar{O}\right)}{\bar{O}} \cdot 100 \tag{5}$$

Table 1
Dataset sources in the UMRB for SWAT setup and simulation.

Data Type	Description	Available Sources	Spatial Resolution
DEM	Shuttle Radar Topography Mission (**SRTM**)	https://earthexplorer.usgs.gov/	90 m
Weather Data	Daily precipitation, maximum/minimum temperature, solar radiation, wind speed, and relative humidity from the NASA North-American Land Data Assimilation System phase 2 (**NLDAS2**)	ldas.gsfc.nasa.gov/nldas/	0.125 °
Land Use	the National Agricultural Statistics Service (NASS). (1) Cropland Data Layer. (2) 2001 National Land Cover Data	nassgeodata.gmu.edu/CropScape	30 m
Soil	the State Soil Geographic (STATSGO) database 1:250,000 scale soil map	websoilsurvey.nrcs.usda.gov	1:250,000
Hydrography	The hydrography GIS layer was from the 2011 National Hydrography Dataset (**NHD**)	nhd.usgs.gov/data.html	1:100,000

Table 2
The five General Climate Models used for climate change simulations with RCP 8.5.

Scenario Dataset	Description	Period
GFDL	Geophysical Fluid Dynamics Laboratory-Earth System Model version 2	1960–2099
HadGEM2	The Hadley centre Global Environmental Model, version 2	1960–2099
IPSL	Institut Pierre-Simon Laplace version 5a, low-resolution configuration	1960–2099
MIROC	(Model for Interdisciplinary Research on Climate, Earth System Model, Chemistry Coupled	1960–2099
NorESM1	Norwegian Earth System Model 1-Medium resolution	1960–2099

where O_i and P_i are observed and simulated values, $\overline{O}$ is the average of the observed,$\overline{P}$is the average of the simulated values. Model performance results are shown in Fig. S1 of the Electronic Supplementary Material.

2.3.2. Model performance on simulating soil thermal status

A previous study compared model performance on simulating daily soil temperature at surface and 5, 10, 20, 50, and 100 cm depths at six stations of the U.S. Climate Reference Network (USCRN) in the UMRB (Qi et al., 2019c). Results show that empirical soil temperature module consistently underestimated winter soil temperatures and overestimated frozen days, while the physically based soil temperature significantly reduced the bias in estimated winter soil temperatures and frozen days. Here, we provided results of simulated vs. observed daily soil temperature at 5 cm depth over the six stations in Fig. S2 of the Electronic Supplementary Material. Details on model comparison and performance improvement can be found in Qi et al. (2019c).

2.4. Model projection and statistical analysis

Simulations driven by the five future climate scenarios were conducted from 1960 to 2099 for both versions of SWAT models. In order to understand the changes in future nitrate loadings in temporal scales, we compared nitrate loadings of each decade of 2000–2099 relative to the baseline period (1960–1999) (Yang et al., 2019). Mean values of annual riverine nitrate loadings for each decade in the 21st century were calculated based on annual simulation results for the five climate scenarios (10 years × 5 scenarios). For the baseline period, the mean value was calculated based on annual loadings simulated with the five climate scenarios (40 years × 5 scenarios). Furthermore, percent changes (%) of annual riverine nitrate loadings for each decade relative to the baseline period were also calculated (= the mean value for a decade / the mean value of the baseline period × 100). The Sen's method was employed to uncover trends in annual riverine nitrate loadings from the baseline period to the end of the 21st century based on mean values as well as percent changes (Sen, 1968). The non-parametric Mann–Kendall (MK) test was adopted to identify the significance in these trends because it does not require data normality (Kendall, 1975; Mann, 1945). The global trend for the entire series is significant when P-value < 0.05.

The MK test and Sen's method were also used to detect trends in climate variables (including precipitation and air temperature), soil thermal status (as indicated by annual frozen days), nitrate loadings (including riverine nitrate loadings, total terrestrial nitrate loadings, and surface and subsurface nitrate loadings as well as nitrate leaching), hydrological variables (including streamflow at the outlet, total terrestrial water yield, and surface and subsurface runoff) and organic nitrogen loadings. Annual frozen days is defined as accumulated days with soil surface temperature < 0 °C with all subbasins divided by the number of subbasins for one year. In addition, the non-parametric Wilcoxon test was used to detect significant difference between simulations by the original SWAT model and SWAT-FT for the baseline period (1960–1999) and each decade of the 21st century (Raje, 2014). We used the Wilcoxon test rather than the *t*-test because simulated hydrologic variables do not follow normal distribution (Raje, 2014). A P-value < 0.05 indicates a significant difference between the two model predictions.

Annual precipitation and average daily air temperature over the UMRB were analyzed based on mean values for each decade from 1960 to 2099. Future climate change trend analysis results are shown in Fig. S3 of the Electronic Supplementary Material. In addition, average annual soil mineral nitrogen transformation fluxes for agriculture lands in the UMRB were calculated for baseline period (1960–1999) and the 21st century (2000–2099) to demonstrate the changes in soil nitrogen cycling processes under future climate change scenarios. The results are shown in Fig. S4 of the Electronic Supplementary Material.

3. Results and discussion

3.1. Responses of soil thermal status to future climate change

Fig. 4a shows annual frozen days decreased as simulated by both models from 1960s to 2090s. The downward trends were attributed to decreasing snow cover extent and depth caused by the warming air temperature as predicted by the five GCMs (Fig. S3). Furthermore, the differences in simulated annual frozen days between the two models were significant (P-value < 0.05) for each period with SWAT-FT having fewer annual frozen days than the original SWAT model (Fig. 4a). This reflects the effects of using the physically based soil temperature module accounting for soil freeze-thaw cycles and snow insulation effects.

The changes of annual frozen days compared with the baseline also show substantial decreases in the 21st century (over −50% by 2090s; Fig. 4b). The original SWAT model projected smaller percent changes than SWAT-FT for all decades, and the differences between the two models expanded with time. The greater changes projected by SWAT-FT are mainly because the physically based soil temperature module is more sensitive to snow cover changes as demonstrated in supplementary Fig. S2 and by previous studies (Qi et al., 2016b, 2019c).

3.2. Future riverine nitrate flux in the UMRB

Overall, both models predicted increasing trends in riverine nitrate fluxes (P-value < 0.05) with SWAT-FT having greater values for the baseline period and each decade of the 21st century (Fig. 5a). SWAT-FT tended to generate more subsurface flow than the original SWAT model (Fig. S9d), because SWAT-FT predicted less annual frozen days (Fig. 5). As a result, more nitrate was leached from root zones and finally exported to streams. Similarly, upward trends in percent changes were detected for both models (P-value < 0.05), but the original SWAT model had greater values (Fig. 5b). The minimum and maximum difference values between the two models occurred in 2000s (2.5%) and 2080s (24.3%), respectively. In general, percent increases predicted by the original SWAT model was about twice the prediction by SWAT-FT by the end of the 21st century (i.e., 2080s and 2090s).

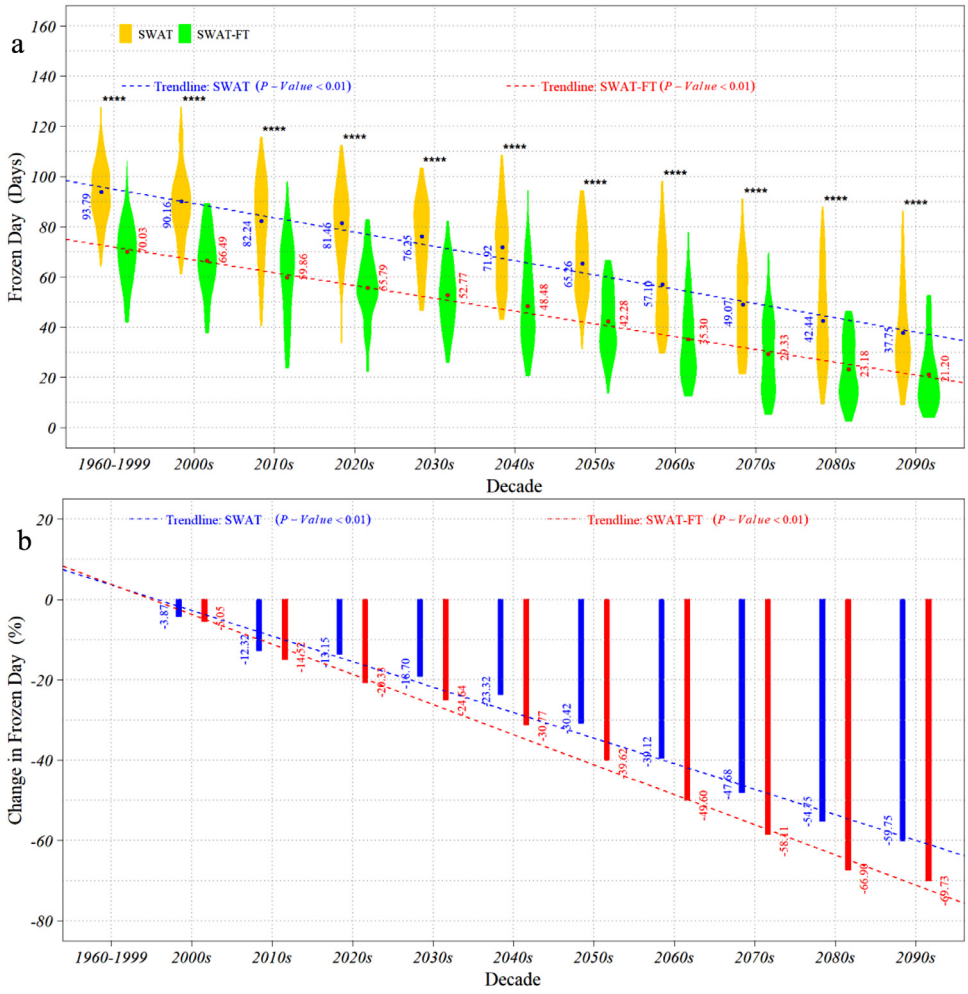

Fig. 4. Mean annual frozen days for the baseline period and each decade of the 21st century (a) and percent change (%) relative to baseline period for each decade in the 21st century (b) simulated by the two versions of SWAT model. "****" indicates P-value < 0.0001. The widths of the violin plot denote probability density of used data.

The results clearly show the sensitivity of nitrate simulation to empirical and physically based representation of freeze-thaw cycle. Employing the original SWAT model to provide guidance for implementation management practices to reduce nitrate loadings from agricultural lands would give inaccurate assessment at the cost of potentially less productivity and more costs on soil and water conservation. For example, a reduction in nitrate loading by 30% has been recommended to reduce hypoxia in the Gulf of Mexico (Mitsch et al., 1999). Using SWAT-FT as a decision support tool would suggest less deployment of best management practices to achieve the goal than the original SWAT model in future climate change scenarios.

3.3. Future terrestrial nitrate loading in the UMRB

Different from the nitrate fluxes which can be monitored at the outlet of a basin, the terrestrial nitrate loading is the summation of the surface nitrate loading and subsurface nitrate loading (= lateral flow nitrate loading + tile flow nitrate loading + baseflow nitrate loading) from uplands (Fig. 2). The terrestrial nitrate loading and its components (surface nitrate loading and subsurface nitrate loading) were the key variables for understanding and unentangling the nitrate cycling processes at the watershed scale and for better design of effective agricultural management practices. We calculated annual terrestrial nitrate loadings, surface nitrate loadings, and subsurface nitrate loadings for the baseline period and each decade of the 21st century (Fig. 6; also see Fig. S6, Fig. S7, and Fig. S8 for reference). There were also upward trends in annual terrestrial nitrate loadings with time (P-value < 0.05) (Figs. 6a and 6d). Like the results for the annual riverine nitrate flux (Fig. 5a), significant differences were observed between the two versions of SWAT model (P-value < 0.05) with SWAT-FT predicting more annual terrestrial nitrate loadings (Fig. 6a). The largest percent change in annual terrestrial nitrate loading relative to the baseline period occur in 2090s (Fig. 6d), with 52.7% projected by the original SWAT model which is nearly twice that of SWAT-FT (29.1%).

To further investigate nitrate cycling processes, the annual surface nitrate loading and subsurface nitrate loading were analyzed. Significant differences in annual surface nitrate loadings predicted by the two versions of SWAT model can be only found before 2060s (Fig. 6b), while there are significant differences in annual subsurface nitrate loading between the two versions of SWAT model for all decades in the 21st century (Fig. 6c). Notably, the differences between the two models for both the surface nitrate loading and subsurface nitrate loading narrowed (Figs. 6b and 6c). The diminishing differences between the two models can be attributed to the decreasing differences in frozen days simulated by the two

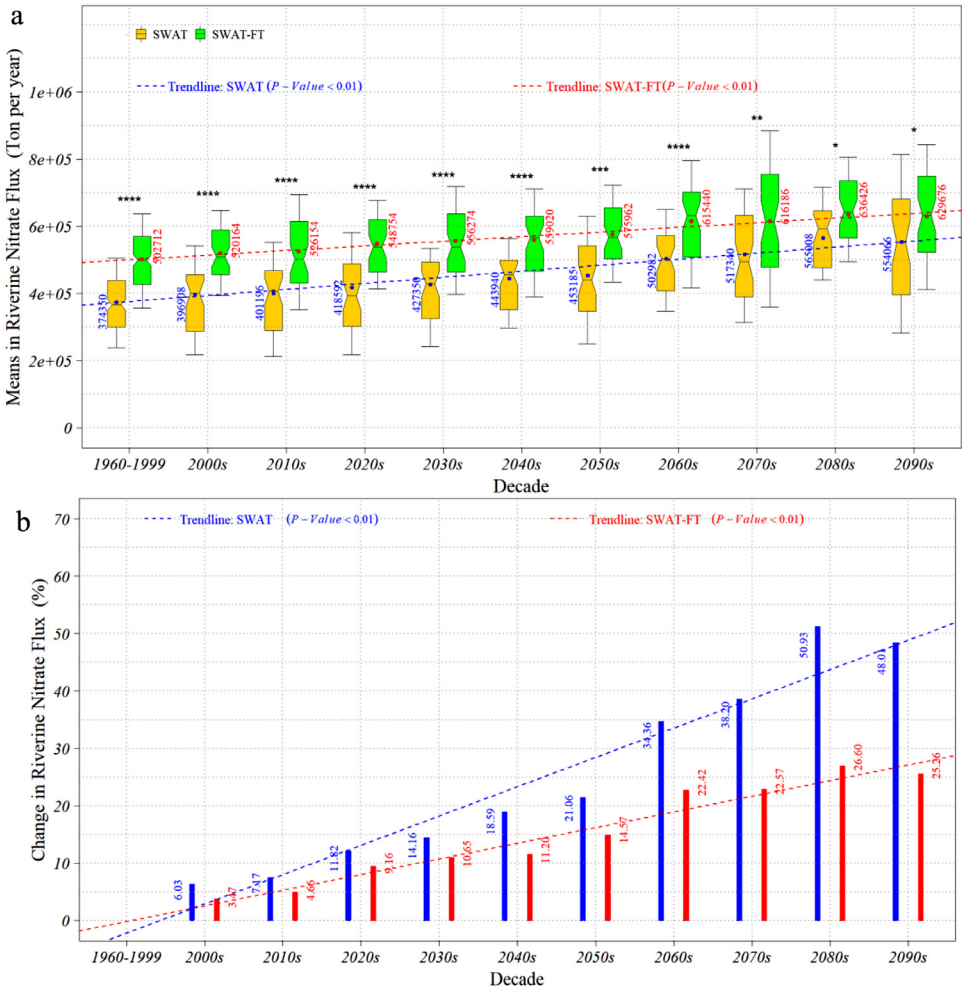

Fig. 5. Mean annual riverine nitrate fluxes at the outlet of the UMRB for the baseline period and each decade of the 21st century (a) and percent change (%) relative to the baseline period (1960–1999) for each decade of the 21st century (b) predicted by the original SWAT model and SWAT-FT. Note that, "****": P-value <= 0.0001, "***": P-value <= 0.001, "**": P-value <= 0.01, and "*": P-value <= 0.05.

models as shown in Fig. 4 (also see Fig. S5). This result shows that the freeze-thaw cycle representation played an important role in prediction of surface nitrate and subsurface nitrate loadings.

The original SWAT model predicted a downward trend in percent changes for the surface nitrate loading (P-value < 0.05) and an upward trend for subsurface nitrate loading (P-value < 0.05) (Figs. 6e and 6f). In contrast, SWAT-FT had an insignificant upward trend for surface nitrate loading (P-value > 0.05) (Fig. 6e), and an upward trend for subsurface nitrate loading. Although the both models predicted an upward trend for subsurface nitrate loading, the trend line of SWAT-FT had a gentler slope than that of the original SWAT model (Fig. 6f). It is worth noting that terrestrial nitrate loading and subsurface nitrate loading exhibit close mean values and slope of percent changes (Figs. 6a, 6c, 6d, and 6f), highlighting the major contribution of subsurface nitrate loading to the total nitrate loading from uplands (Figs. 6b and 6c). The significance of subsurface nitrate loading requires accurate simulation of hydrological processes impacted by soil thermal status, thereby accentuating the important role of freeze-thaw cycles in hydrological modeling.

3.4. Spatial variability in surface and subsurface nitrate loading in the umrb

Information on spatial variability of surface and subsurface nitrate loading components is essential for water quality management, agricultural management, and implementation of adaptation strategies at the watershed scale. To better clarify the effects of soil freeze-thaw cycle on nitrate loadings in projected future climate conditions, we calculated the spatial differences (= simulations by the original SWAT model minus simulations by SWAT-FT for each subbasin) of average annual surface and subsurface nitrate loadings in the UMRB for four periods (Fig. 7), including the baseline period (1960–1999) and three future 30-year periods (i.e., 2010–2039, 2040–2069, and 2070–2099 representing near term, mid-term, and long-term future conditions). In most subbasins, differences in the surface nitrate loading were positive indicating that surface nitrate loading predicted by the original SWAT model was greater than that of SWAT-FT, except for several southern subbasins (Fig. 7a). The differences in the surface nitrate loading predicted by the two models tended to decrease over time. Note that the range of the

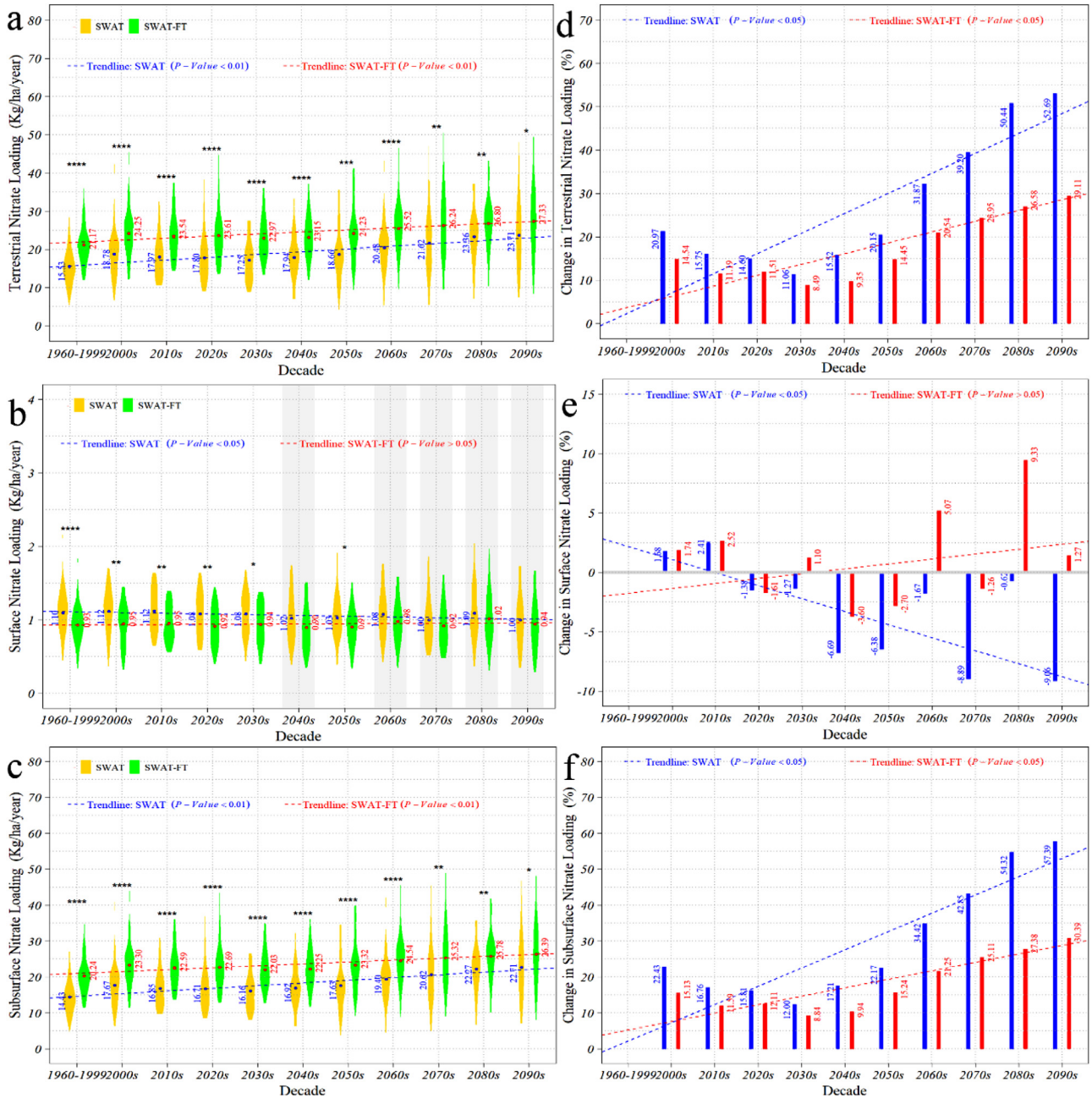

Fig. 6. Mean annual terrestrial nitrate loading (a), surface nitrate loading (b), and subsurface nitrate loading (c) predicted by the original SWAT model and SWAT-FT and corresponding percentage change (%) for each decade of the 21st century (d, e, and f for terrestrial nitrate loading, surface nitrate loading, and subsurface nitrate loading, respectively). Note that "****": P-value <= 0.0001, "***": P-value <= 0.001, "**": P-value <= 0.01, and "*": P-value <= 0.05. Vertical gray strips denote P-value > 0.05. The widths of the violin plot denote probability density of the used data.

differences between surface nitrate loading simulated by the two models was between −1 and 1 kg ha^{-1} yr^{-1} which is almost negligible compared to the total terrestrial nitrate loading.

Differences between subsurface nitrate loadings predicted by the two models were negative (Fig. 7a), indicating that the original SWAT model predicted less subsurface nitrate loadings than SWAT-FT across the basin (Fig. 7b). We also found the differences in subsurface nitrate loadings between the two model are larger in northwestern subbasins (maximum difference of about −15 kg ha^{-1} year^{-1}) than in the southeastern subbasins. In addition, the differences in subsurface nitrate loadings also tended to narrow over time which is consistent with previous temporal analyses (also see Fig. 6c). The cause of the narrowing difference between simulated surface and subsurface nitrate loadings predicted by the two versions of SWAT model is mainly attributed to the narrowing difference in simulated frozen days (Fig. 4a).

Detailed information on spatial characteristics of nitrate loadings associated with subbasins can help decision making to implement effective management practices to reduce nitrate leaching and improve water quality in streams (Shaffer et al., 1991). As northern UMRB experiences more intensive freeze-thaw cycle and the original SWAT model and SWAT-FT exhibited larger differences in the colder region, it is deserved to pay more attention to those

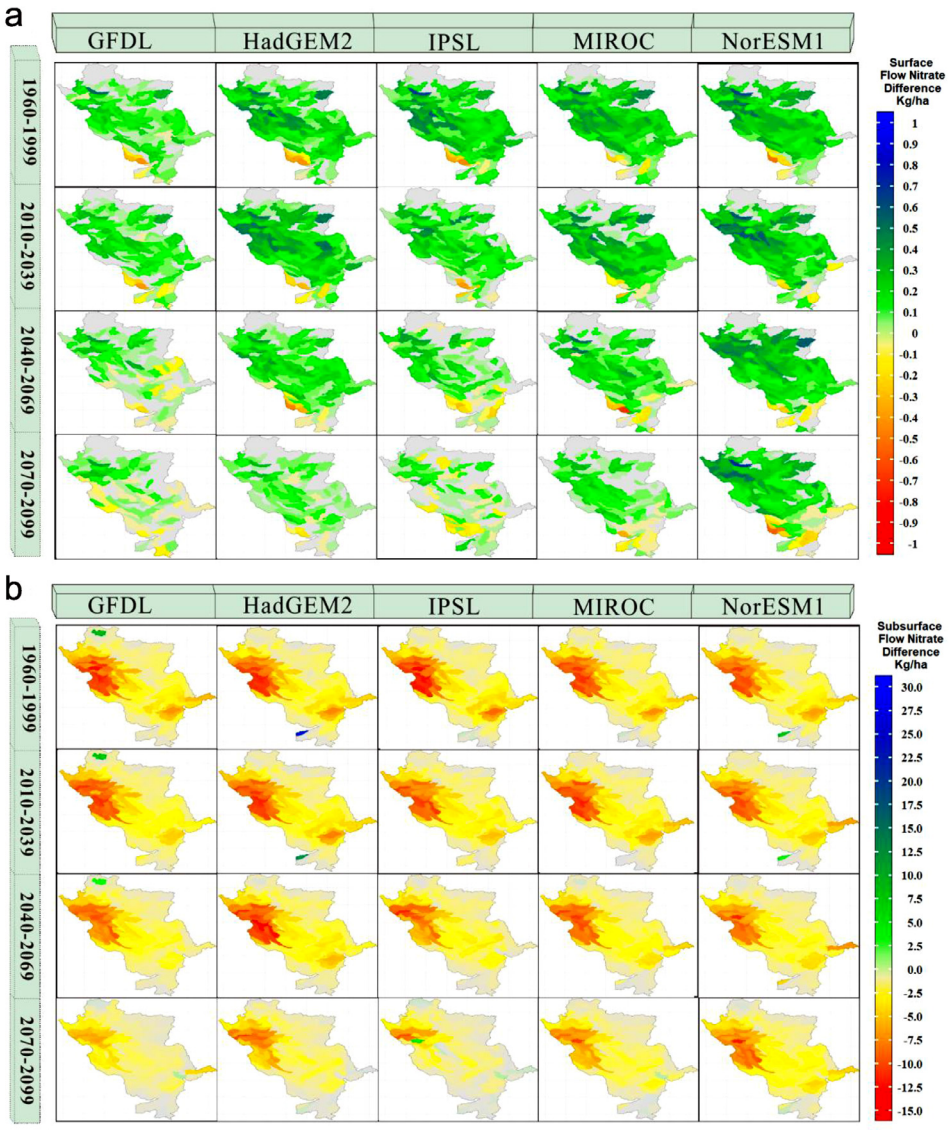

Fig. 7. Spatial distribution of the difference between predicted average annual terrestrial surface (a) and subsurface (b) nitrate loadings by the original SWAT model and SWAT-FT during four periods using five different GCMs.

vulnerable areas when designing mitigation strategies under future climate change conditions.

3.5. Future nitrate leaching and organic nitrogen loading

We also provided the projection on annual nitrate leaching and terrestrial organic nitrogen loading for baseline period and each decade of the 21st century as shown in Figs. S10–11 and Fig. S12, respectively, in the Electronic Supplementary Material. Model projection on annual nitrate leaching had similar trends to the total subsurface nitrate loading for both models (Figs. 6c and 6f vs. Figs. S10a and S10b), which is understandable because nitrate leaching contributes greatly to the subsurface nitrate loading (Fig. 2). Model projection on annual organic nitrogen loading showed significant decreasing trends for both models (Figs. S12a and S12b), which was consistent with the decreasing trend in surface runoff of the original SWAT model (Fig. S9c), but not for SWAT-FT whose annual surface runoff had insignificant trend (P-value $>$ 0.05). The different association between annual surface runoff and organic nitrogen loading for the original SWAT model and SWAT-FT implied the sensitivity of organic matter loading projection to freeze-thaw cycle representation, which is out of scope of this study.

3.6. Relation between nitrate loading and water flow

Figure S9 shows model projections on annual stream flow at the outlet, total terrestrial water yield in the UMRB, and surface and subsurface runoff for both models for baseline period and each decade of the 21st century. Contrary to riverine nitrate flux and total terrestrial nitrate loading, there were no significant differences in annual stream flow and water yield between the two SWAT models for different periods (P-value $>$ 0.05; Figs. S9a and S9b). Like surface and subsurface nitrate loadings, there were also significant differences between two models for surface and subsurface runoff (Figs. S9c and S9d). Except for surface runoff, changing trends in annual stream flow, water yield, and subsurface runoff were opposite to respective nitrate loadings for both models. The downward trends of stream flow, water yield, and

subsurface runoff were caused by the increasing ET in the UMRB (Wang et al., 2020), while the upward trends of riverine nitrate flux, total terrestrial nitrate loading, and subsurface nitrate loading were due to increased nitrate concentration in soil profile caused by accelerated mineralization and nitrification rates under future warmer conditions (Dai et al., 2020). For the annual surface runoff, it had the similar changing trends to the annual surface nitrate loading projected by both models with the original SWAT model having decreasing trends in surface runoff and surface nitrate loading, and SWAT-FT having insignificant changing trends (P-value >0.05; Fig. S9c vs Fig. 6b) .

4. Conclusions

With improved freeze-thaw cycle representation, SWAT-FT better simulated soil thermal status, streamflow, and riverine nitrate fluxes in the UMRB. Driven by five GCMs under the RCP8.5 scenario, both SWAT-FT and the original SWAT model projected increases in terrestrial nitrate loadings in the 21st century, with SWAT-FT predicting higher loadings due to more subsurface nitrate contributions caused by less predicted frozen days.

Compared with the baseline period of 1960–1999, the original SWAT model predicted a 50% increase of total nitrate loadings from uplands at the end of the 21st century which was about twice that predicted by SWAT-FT (ca. 25%). The large differences between projected future relative changes (ca. 50% by the original SWAT model vs. ca. 25% by SWAT-FT) highlight the relevance of freeze-thaw cycle representation to effective design of water quality management practices to reduce nitrate fluxes from URMB (e.g. 30% reduction as suggested by Mitsch et al., 1999).

Spatial distribution of surface and subsurface nitrate loading from upland also showed that major differences between the original SWAT model and SWAT-FT exist in the northern UMRB, which experiences more intensive freeze-thaw cycle than the southern part. Overall, our results clearly show the sensitive responses of upland nitrate loading and riverine nitrate fluxes to different freeze-thaw cycle representation. The use of physically based freeze-thaw cycle representation in water quality modeling is important for reliable assessment of future water quality improvement efforts under climate change.

The present study considered constant atmospheric reactive nitrogen deposition rate and CO_2 concentration for future hydrology and water quality modeling in the UMRB. Terrestrial emissions to the atmosphere and the feedback to land surface ecosystems are also important for climate change studies. Future research is needed to consider these complex processes by coupling SWAT-FT with climate models to reduce prediction uncertainty.

Declaration of Competing Interest

The authors declare that they have no known competing financial interests or personal relationships that could have appeared to influence the work reported in this paper.

Acknowledgement

We greatly appreciate the comments from four anonymous reviewers, which helped us to improve the quality of our paper. Drs. Xuesong Zhang and Junyu Qi were partially supported by National Science Foundation (1639327). Disclosure: The views expressed in this paper are those of the authors and do not necessarily represent the views or policies of the U.S. Environmental Protection Agency.

Supplementary materials

Supplementary material associated with this article can be found, in the online version, at doi:10.1016/j.watres.2020.116355.

References

Alexander, R.B., Schwarz, G.E., Smith, R.A., 1997. Regional transport of point and nonpoint-source nitrogen to the gulf of Mexico. Gulf of Mexico Program Office.
Bakir, M., Zhang, X., 2008. GIS-based hydrological modelling: a comparative study of HEC-HMS and the Xinanjiang model. IAHS Publ.-Series Proc. Rep. 319, 124–133.
Borah, D., Bera, M., 2003. Watershed-scale hydrologic and nonpoint-source pollution models: review of mathematical bases. Transactions of the ASAE 46 (6), 1553.
Buytaert, W., Vuille, M., Dewulf, A., Urrutia, R., Karmalkar, A., Célleri, R., 2010. Uncertainties in climate change projections and regional downscaling in the tropical Andes: implications for water resources management. Hydrol. Earth Syst. Sci. 14 (7), 1247.
Dai, Z., Yu, M., Chen, H., Zhao, H., Huang, Y., Su, W., Xia, F., Chang, S.X., Brookes, P.C., Dahlgren, R.A., 2020. Elevated temperature shifts soil N cycling from microbial immobilization to enhanced mineralization, nitrification and denitrification across global terrestrial ecosystems. Glob. Change Biol..
Deb, D., Tuppad, P., Daggupati, P., Srinivasan, R., Varma, D., 2015. Spatio-temporal impacts of biofuel production and climate variability on water quantity and quality in upper Mississippi river basin. Water (Basel) 7 (7), 3283–3305.
Guo, D., Wang, H., 2013. Simulation of permafrost and seasonally frozen ground conditions on the Tibetan Plateau, 1981–2010. J. Geophys. Res.: Atmos. 118 (11), 5216–5230.
Hagemann, S., Chen, C., Clark, D.B., Folwell, S., Gosling, S.N., Haddeland, I., Hanasaki, N., Heinke, J., Ludwig, F., Voss, F., 2013. Climate change impact on available water resources obtained using multiple global climate and hydrology models. Earth Syst. Dyn. 4 (1), 129–144.
Hentschel, K., Borken, W., Matzner, E., 2008. Repeated freeze–thaw events affect leaching losses of nitrogen and dissolved organic matter in a forest soil. J. Plant Nutr. Soil Sci. 171 (5), 699–706.
Hillel, D., 1980. Fundamentals of soil physics. Inc.(London) Ltd. Academic Press.
Johansen, O. (1975) Thermal conductivity of soils. Ph.D., Trondheim, Norway (CRREL Draft Translation 637, 1977) ADA 044002.
Kendall, C., 1998. Isotope Tracers in Catchment Hydrology. Elsevier, pp. 519–576.
Kendall, M., 1975. In: Rank Correlation Measures, 202. Charles Griffin, London, p. 15.
Kimball, J.S., McDonald, K., Keyser, A.R., Frolking, S., Running, S.W., 2001. Application of the NASA scatterometer (NSCAT) for determining the daily frozen and nonfrozen landscape of Alaska. Remote Sens Environ 75 (1), 113–126.
Mann, H., 1945. Non-parametric tests against trend. Econmetrica 13, 245–259.
Middelkoop, H., Daamen, K., Gellens, D., Grabs, W., Kwadijk, J.C., Lang, H., Parmet, B.W., Schädler, B., Schulla, J., Wilke, K., 2001. Impact of climate change on hydrological regimes and water resources management in the Rhine basin. Clim. Change 49 (1–2), 105–128.
Miller, M.P., Tesoriero, A.J., Hood, K., Terziotti, S., Wolocks, D.M., 2017. Estimating discharge and nonpoint source nitrate loading to streams from three end-member pathways using high-frequency water quality data. Water Resour. Res. 53 (12), 10201–10216.
Mitsch, W.J., Day, J.W., Gilliam, J.W., Groffman, P.M., Hey, D.L., Randall, G.W. and Wang, N. 1999. Reducing nutrient loads, especially nitrate-nitrogen, to surface water, ground water, and the Gulf of Mexico: topic 5 report for the integrated assessment on hypoxia in the Gulf of Mexico.
Moriasi, D.N., Gowda, P.H., Arnold, J.G., Mulla, D.J., Ale, S., Steiner, J.L., 2013. Modeling the impact of nitrogen fertilizer application and tile drain configuration on nitrate leaching using SWAT. Agric. Water Manage. 130, 36–43.
Nash, J.E., Sutcliffe, J.V., 1970. River flow forecasting through conceptual models part I—A discussion of principles. J. Hydrol. (Amst) 10 (3), 282–290.
Neitsch, S.L., Arnold, J.G., Kiniry, J.R., Williams, J.R., 2011a. Soil and Water Assessment Tool Theoretical Documentation Version 2009. Texas Water Resources Institute.
Neitsch, S.L., Williams, J.R., Arnold, J.G., Kiniry, J.R., 2011b. Soil and Water Assessment Tool Theoretical Documentation Version 2009. Grassland, Soil and Water Research Service, Temple, Texas, USA.
Nunes, J.P., Seixas, J., Pacheco, N.R., 2008. Vulnerability of water resources, vegetation productivity and soil erosion to climate change in Mediterranean watersheds. Hydrol. Process.: Int. J. 22 (16), 3115–3134.
Ouyang, W., Huang, H., Hao, F., Guo, B., 2013. Synergistic impacts of land-use change and soil property variation on non-point source nitrogen pollution in a freeze–thaw area. J. Hydrol. (Amst) 495, 126–134.
Panagopoulos, Y., Gassman, P., Arritt, R., Herzmann, D., Campbell, T., Jha, M.K., Kling, C., Srinivasan, R., White, M., Arnold, J., 2014. Surface water quality and cropping systems sustainability under a changing climate in the Upper Mississippi river basin. J. Soil Water Conserv. 69 (6), 483–494.
Parton, W., Mosier, A., Ojima, D., Valentine, D., Schimel, D., Weier, K., Kulmala, A.E., 1996. Generalized model for N2 and N2O production from nitrification and denitrification. Global Biogeochem. Cycles 10 (3), 401–412.
Plan, G.H.A. 2008. For reducing, mitigating, and controlling hypoxia in the northern Gulf of Mexico and improving water quality in the Mississippi river basin. Mississippi River Gulf of Mexico Watershed Nutrient Task Force, US Environmental Protection Agency, Office of Wetlands, Oceans, and Watersheds: Washington, DC.

Qi, J., Li, S., Li, Q., Xing, Z., Bourque, C.P.-A., Meng, F.-R., 2016a. Assessing an enhanced version of SWAT on water quantity and quality simulation in regions with seasonal snow cover. Water Resour. Manage. 30 (14), 5021–5037.
Qi, J., Li, S., Li, Q., Xing, Z., Bourque, C.P.-A., Meng, F.-R., 2016b. A new soil-temperature module for SWAT application in regions with seasonal snow cover. J Hydrol (Amst) 538, 863–877.
Qi, J., Wang, Q., Zhang, X., 2019a. On the Use of NLDAS2 weather data for hydrologic modeling in the upper Mississippi river basin. Water (Basel) 11 (5), 960.
Qi, J., Zhang, X., Cosh, M.H., 2019b. Modeling soil temperature in a temperate region: a comparison between empirical and physically based methods in SWAT. Ecol. Eng. 129, 134–143.
Qi, J., Zhang, X., Wang, Q., 2019c. Improving hydrological simulation in the upper Mississippi river basin through enhanced freeze-thaw cycle representation. J. Hydrol. (Amst) 571, 605–618.
Qi, J., Zhang, X., Yang, Q., Srinivasan, R., Arnold, J.G., Li, J., Waldholf, S.T., Cole, J., 2020. SWAT ungauged: water quality modeling in the upper Mississippi river basin. J. Hydrol. (Amst), 124601.
Rabalais, N.N., Turner, R.E., JustiĆ, D., Dortch, Q., Wiseman, W.J., Gupta, B.K.S., 1996. Nutrient changes in the Mississippi River and system responses on the adjacent continental shelf. Estuaries 19 (2), 386–407.
Raje, D., 2014. Changepoint detection in hydrologic series of the Mahanadi River basin using a Fuzzy Bayesian approach. J. Hydrol. Eng. 19 (4), 687–698.
Schindler, D.W., 2012. The dilemma of controlling cultural eutrophication of lakes. Proc. R. Soc. B: Biol. Sci. 279 (1746), 4322–4333.
Sen, P.K., 1968. Estimates of the regression coefficient based on Kendall's tau. J Am Stat Assoc 63 (324), 1379–1389.
Shaffer, M., Halvorson, A., Pierce, F., 1991. Nitrate leaching and economic analysis package (NLEAP): model description and application. Manag. Nitrogen Groundwater Q. Farm Profitab. 285–322.
Srinivasan, R., Zhang, X., Arnold, J., 2010. SWAT ungauged: hydrological budget and crop yield predictions in the upper Mississippi river basin. Trans. ASABE 53 (5), 1533–1546.
Steppuhn, H. 1981. Snow and agriculture. Handbook of snow, principles, processes, management and use. Pergamon, Toronto, 60–126.
Sturm, M., Holmgren, J., König, M., Morris, K., 1997. The thermal conductivity of seasonal snow. J. Glaciol. 43 (143), 26–41.
Verseghy, D.L., 1991. CLASS—A Canadian land surface scheme for GCMs. I. Soil model. Int. J. Climatol. 11 (2), 111–133.
Wang, Q., Qi, J., Wu, H., Zeng, Y., Shui, W., Zeng, J., Zhang, X., 2020. Freeze-thaw cycle representation alters response of watershed hydrology to future climate change. Catena 195, 104767.
Wu, H., Adler, R.F., Tian, Y., Huffman, G.J., Li, H., Wang, J., 2014. Real-time global flood estimation using satellite-based precipitation and a coupled land surface and routing model. Water Resour. Res. 50 (3), 2693–2717.
Wu, M., Demissie, Y., Yan, E., 2012. Simulated impact of future biofuel production on water quality and water cycle dynamics in the upper Mississippi river basin. Biomass Bioenerg. 41, 44–56.
Wu, Y., Ouyang, W., Hao, Z., Lin, C., Liu, H., Wang, Y., 2018. Assessment of soil erosion characteristics in response to temperature and precipitation in a freeze-thaw watershed. Geoderma 328, 56–65.
Yang, M., Yao, T., Gou, X., Hirose, N., Fujii, H.Y., Hao, L., Levia, D., 2007. Diurnal freeze/thaw cycles of the ground surface on the Tibetan Plateau. Chin. Sci. Bull. 52 (1), 136–139.
Yang, Q., Zhang, X., Abraha, M., Del Grosso, S., Robertson, G., Chen, J., 2017. Enhancing the soil and water assessment tool model for simulating N2O emissions of three agricultural systems. Ecosyst. Health Sustain. 3 (2), e01259.
Yang, Q., Zhang, X., Almendinger, J.E., Huang, M., Chen, X., Leng, G., Zhou, Y., Zhao, K., Asrar, G.R., Li, X., 2019. Climate change will pose challenges to water quality management in th. . Environ. Pollut. 251, 302–311.
Yi, J., Zhao, Y., Shao, M.a., Zhang, J., Cui, L., Si, B., 2014. Soil freezing and thawing processes affected by the different landscapes in the middle reaches of Heihe River Basin, Gansu, China. J Hydrol (Amst) 519, 1328–1338.
Yu, X., Zou, Y., Jiang, M., Lu, X., Wang, G., 2011. Response of soil constituents to freeze–thaw cycles in wetland soil solution. Soil Biol. Biochem. 43 (6), 1308–1320.
Zhang, T., 2005. Influence of the seasonal snow cover on the ground thermal regime: an overview. Rev. Geophys. 43 (4).
Zhang, X., 2018. Simulating eroded soil organic carbon with the SWAT-C model. Environ. Model. Softw. 102, 39–48.
Zhang, X., Izaurralde, R.C., Arnold, J.G., Williams, J.R., Srinivasan, R., 2013. Modifying the soil and water assessment tool to simulate cropland carbon flux: model development and initial evaluation. Sci. Total Environ. 463, 810–822.
Zhang, X., Srinivasan, R., Debele, B., Hao, F., 2008a. Runoff simulation of the headwaters of the yellow river using The SWAT model with three snowmelt algorithms 1. JAWRA J. Am. Water Resour. Assoc. 44 (1), 48–61.
Zhang, X., Sun, S., 2011. The impact of soil freezing/thawing processes on water and energy balances. Adv. Atmos. Sci. 28 (1), 169–177.
Zhang, Z., Fukushima, T., Shi, P., Tao, F., Onda, Y., Gomi, T., Mizugaki, S., Asano, Y., Kosugi, K.i, Hiramatsu, S., 2008b. Baseflow concentrations of nitrogen and phosphorus in forested headwaters in Japan. Sci. Total Environ. 402 (1), 113–122.
Zhang, Z., Fukushima, T., Shi, P., Tao, F., Onda, Y., Gomi, T., Mizugaki, S., Asano, Y., Kosugi, K.i, Hiramatsu, S., 2008c. Seasonal changes of nitrate concentrations in baseflow headwaters of coniferous forests in Japan: a significant indicator for N saturation. Catena 76 (1), 63–69.
Zhao, Y., Huang, M., Horton, R., Liu, F., Peth, S., Horn, R., 2013. Influence of winter grazing on water and heat flow in seasonally frozen soil of Inner Mongolia. Vadose Zone J. 12 (1).